



	<b>Experiment title: Self-assembly of low molecular weight and polymeric materials for organic electronic devices</b>	<b>Experiment number:</b> SC2647
<b>Beamline:</b> ID02	<b>Date of experiment:</b> from: 19.6.09 to: 22.6.09	<b>Date of report:</b> 27.8.2009
<b>Shifts:</b> 9	<b>Local contact(s):</b> Michael Stzucki	<i>Received at ESRF:</i>
<b>Names and affiliations of applicants (* indicates experimentalists):</b>  Sven Huettnner*, Cavendish Laboratory, University of Cambridge & Applied Functional Polymers, Universität Bayreuth  Dr. Michael Sommer*, Applied Functional Polymers, Universität Bayreuth  Prof. Ullrich Steiner, Cavendish Laboratory, University of Cambridge  Prof. Mukundan Thelakkat, Applied Functional Polymers, Universität Bayreuth  <u>Further experimentalists:</u> Dr. Peter Kohn*, Universität Halle Mathias Kolle*, Cavendish Laboratory University of Cambridge Heiko Schoberth*, Physikalische Chemie II, Universität Bayreuth		

## Report:

We have investigated several n-type low molecular weight and polymeric systems suitable for the application in organic electronic devices such as organic field-effect transistors (OFET) or organic photovoltaics (OPV). The materials investigated include:

- 1) A symmetrically substituted low molecular weight perylene bisimide (SL123)
- 2) An asymmetrically substituted low molecular weight perylene benzimidazole (AW73)
- 3) A side-chain crystalline perylene bisimide homopolymer, referred to as PPerAcr
- 4) Amorphous-crystalline block copolymers comprised of polystyrene and PPerAcr (PS-*b*-PPerAcr)
- 5) Double crystalline and fully functionalized block copolymers comprised of poly(hexylthiophene) (P3HT) and PPerAcr (P3HT-*b*-PPerAcr).

While the first two low molecular weight compounds are discotic liquid crystals, the latter two are side-chain crystalline perylene bisimide moieties. In all cases, a supramolecular arrangement is observed. We have measured temperature-dependent phase transitions between room temperature and the isotropic melt of compounds 1-3, which allows a precise determination of the internal structure of these materials. The chemical structures of these compounds are depicted in figure 1. The fourth system investigated is a series of amorphous-crystalline block copolymers PS-*b*-PPerAcr 4 with different compositions and different molecular weights.

Since the self-assembling process of these materials is complex, our investigation starts with the self-assembly of the basic chromophores (SL123, AW73). In a next step, we investigate structure formation of the homopolymer PPerAcr, in which these chromophores are tied to a polyacrylate backbone. Finally, a series of block copolymers with PPerAcr and a soft, amorphous polystyrene block is investigated (figure 1) and an outlook on fully functionalized block copolymers that are made for the application in organic solar cells is given.

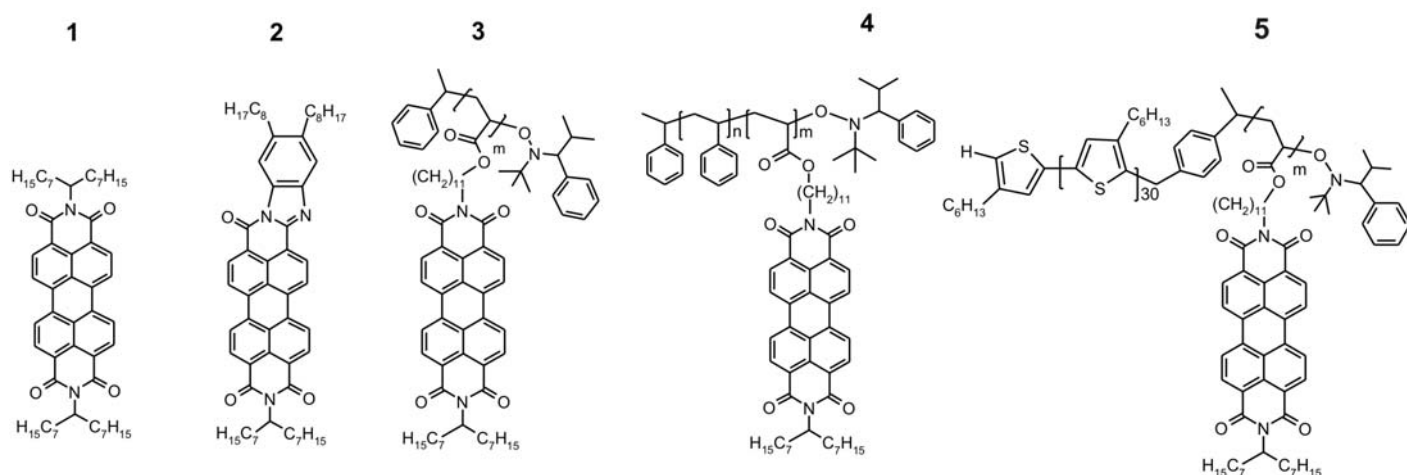


Figure 1. Chemical structures of the investigated n-type low molecular weight perylene bisimide 1, perylene benzimidazole 2, poly(peryene bisimide acrylate) PPerAcr 3, polystyrene-*block*-poly(peryene bisimide acrylate) PS-*b*-PPerAcr 4 and poly(hexylthiophene)-*block*- poly(peryene bisimide acrylate) P3HT-*b*-PPerAcr 5

The phase behaviour of PS-*b*-PPerAcr is governed by crystallization, main-chain side-chain segregation, and microphase separation. Those materials self-assemble on different length scales between 0.3 and 30 nm. The different levels of structure formation are schematically shown in figure 2.

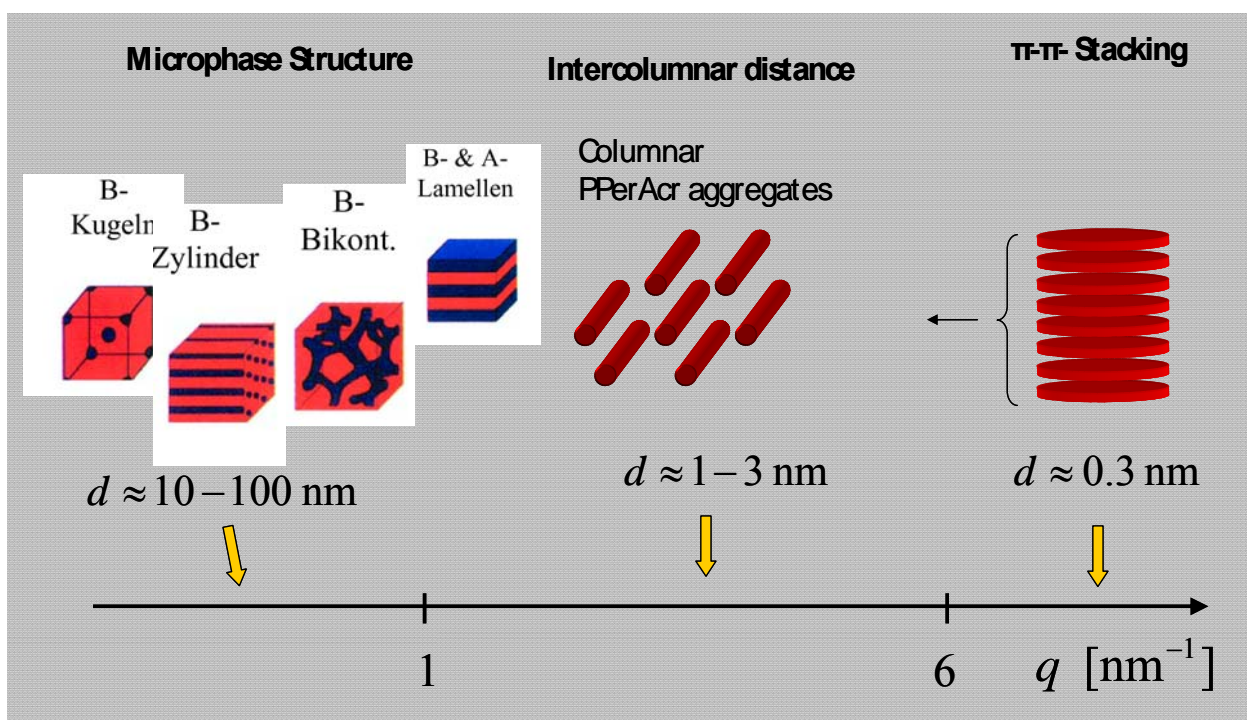


Figure 2. Different hierarchies of structure formation in PS-*b*-PPerAcr 4. The perylene bisimide moieties form  $\pi$ - $\pi$  stacks with a typical distance of 0.35 nm. These  $\pi$ - $\pi$  stacks or columns are packed within microdomains that are separated by polystyrene.

All experimentalists totally agree that the beamtime was a major success since many questions were addressed and solved. During the measurements we have also addressed questions such as reproducibility of results and beam damage (several heating and cooling cycles).

In addition, we have successfully tested a novel sample holder geometry that allows us to conduct temperature-dependent SAXS/WAXS measurements on free-standing bulk samples with minimum amounts of material (~1-2 mg). This is important owing to the small amounts of material available (resulting from the large number of synthetic steps) and consequently opened the door to us for further measurements at ID02.

The following pages collect the most important diffraction pattern and conclusions. While we have measured several heating and cooling cycles of each compound, we show here only the diffraction patterns acquired during the cooling process. Classification is made according to the five points mentioned above. However, due to the large body of data created, the complete evaluation and indexing of all data will take more time.

### 1) Symmetrically substituted low molecular weight perylene bisimide SL123

Ambiguity exists over the internal structure of symmetrically substituted perylene bisimides with two branched swallow-tail alkyl substituents (SL123). While a orthorhombic unit cell has been proposed first by X-ray scattering experiments<sup>1</sup> and molecular dynamic simulations<sup>2</sup>, a monoclinic unit cell was reported lateron.<sup>3</sup> Furthermore, several reports exists in which the compound exhibits only one transition from the crystalline to the isotropic phase. However, a liquid crystalline phase has also been observed. We have measured SL123 temperature dependent. An example of the room temperature diffraction pattern is shown in figure 3.

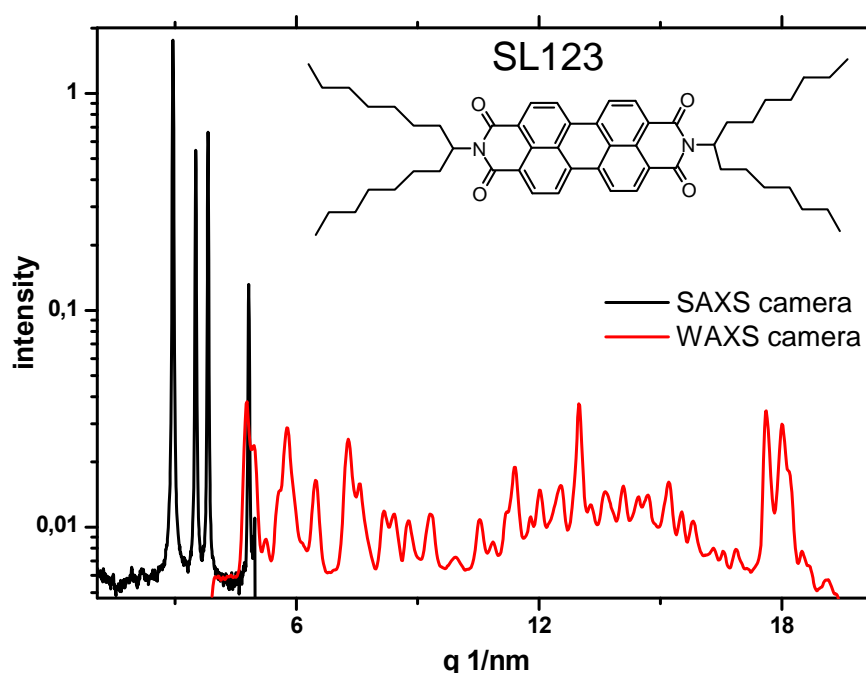


Figure 3. Combined SAXS/WAXS diffraction pattern of a bulk sample of low molecular weight perylene bisimide SL123 at room temperature.

<sup>1</sup> Nolde, F.; Pisula, W.; Müller, S.; Kohl, C.; Müllen, K. *Chem. Mater.* **2006**, *18*, 3715.

<sup>2</sup> Marcon, V.; Kirkpatrick, J.; Pisula, W.; Andrienko, D. *Phys. Status Solidi B* **2008**, *245*, 820.

<sup>3</sup> Marcon, V.; Breiby, D. W.; Pisula, W.; Dahl, J.; Kirkpatrick, J.; Patwardhan, S.; Grozema, F.; Andrienko, D. *JACS*, article ASAP, doi: 10.1021/ja900963v

The evaluation of these data as well as the temperature-dependent diffraction pattern will not only bring clarity to the confusion of statements in the literature, but also serve as a starting point for investigating the self-assembling process in side-chain crystalline polymers.

## 2) Unsymmetrically substituted perylene benzimidazole AW73

Another n-type building block among perylene bisimides are perylene benzimidazoles. Due to the strong  $\pi$ - $\pi$  interactions these compounds are commonly processed by vacuum sublimation when unsubstituted. Here we investigate the structure formation of a novel soluble unsymmetric perylene benzimidazole derivative which can be processed from solution. Figure 4a,b show a series of scattering curves recorded during the first cooling cycle. Figures 4c-f enlarge different regions of the  $q$ -range.

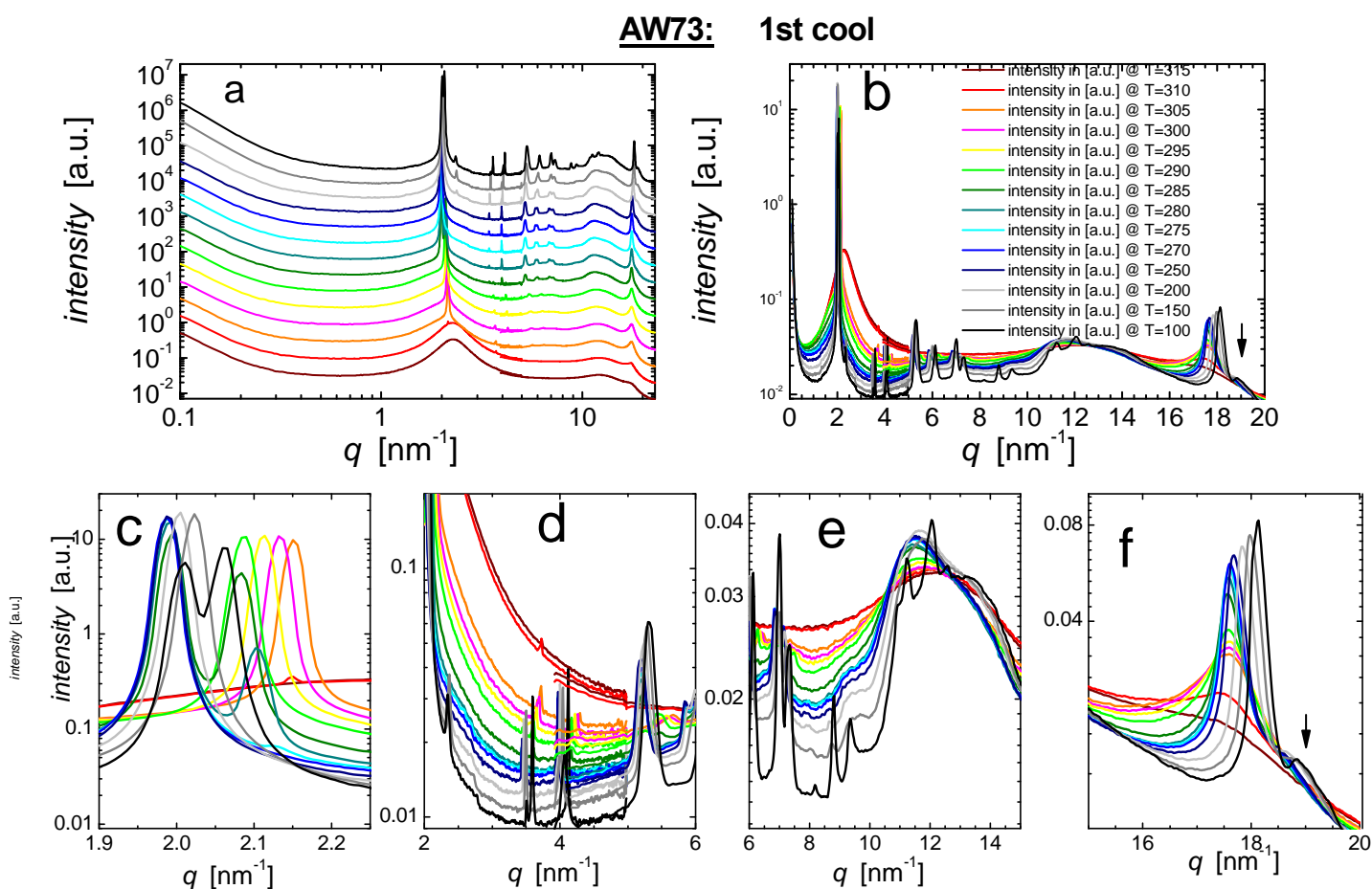


Figure 4. Combined SAXS/WAXS diffraction patterns of a bulk sample of AW73 during cooling at 10 K/min.

Since we investigated here a novel substance, we were mainly interested in the phase behavior of this molecule. Upon cooling from the isotropic liquid, we first observe a columnar disordered phase, i.e. the molecules form columns on a 2-d lattice, but are packed liquid-like within the columns. The observation of a peak in the small angle region (Fig.4c, e.g orange line) indicates the formation of columns, while the broad reflection in Fig.4f at higher temperatures is indicative for a short range ordering of the plate-like molecules

within the columns. Further cooling leads to a phase transition to a columnar ordered phase: higher order reflections are observed in the small angle region (Fig 4c, d,e) and the pronounced sharpening of the reflection in Fig.4f indicate a crystal like packing within the columns. Furthermore reflections at higher  $q$ -values are observed and indicated by arrows in Figs.4b and 4f. These reflections are Bragg-reflections with mixed  $hkl$  indices, where  $h$  and  $k$  are related to the 2d lattice of the columns and  $l$  to the ordering within the columns. In this phase the discotic molecules are therefore arranged on a 3d lattice. During the phase transition from the disordered to the ordered phase, e.g. olive and cyan line in Fig. 4c, there seems to exist a coexistence of the two phases. Further detailed analysis of the lattice type and the phase transition and the phase coexistence is underway to fully clarify the process of structure formation.

### 3) Side-chain crystalline poly(perylene bisimide acrylate) PPerAcr

This side-chain crystalline n-type polymer has been used as n-type material in amorphous-crystalline<sup>4, 5, 6</sup>, as well as in double crystalline<sup>7</sup> block copolymers for photovoltaic cells. However, the exact structure of PPerAcr is currently unknown. Here we aim to determine its structure and phase transitions. We also measured samples that experienced a different history (solvent annealing, temperature treatment below the melting point). Figure 5a shows a series of diffraction patterns of a cool down from the melt at 10 K/min, and figures b)-d) enlarge different regions of the  $q$ -range.

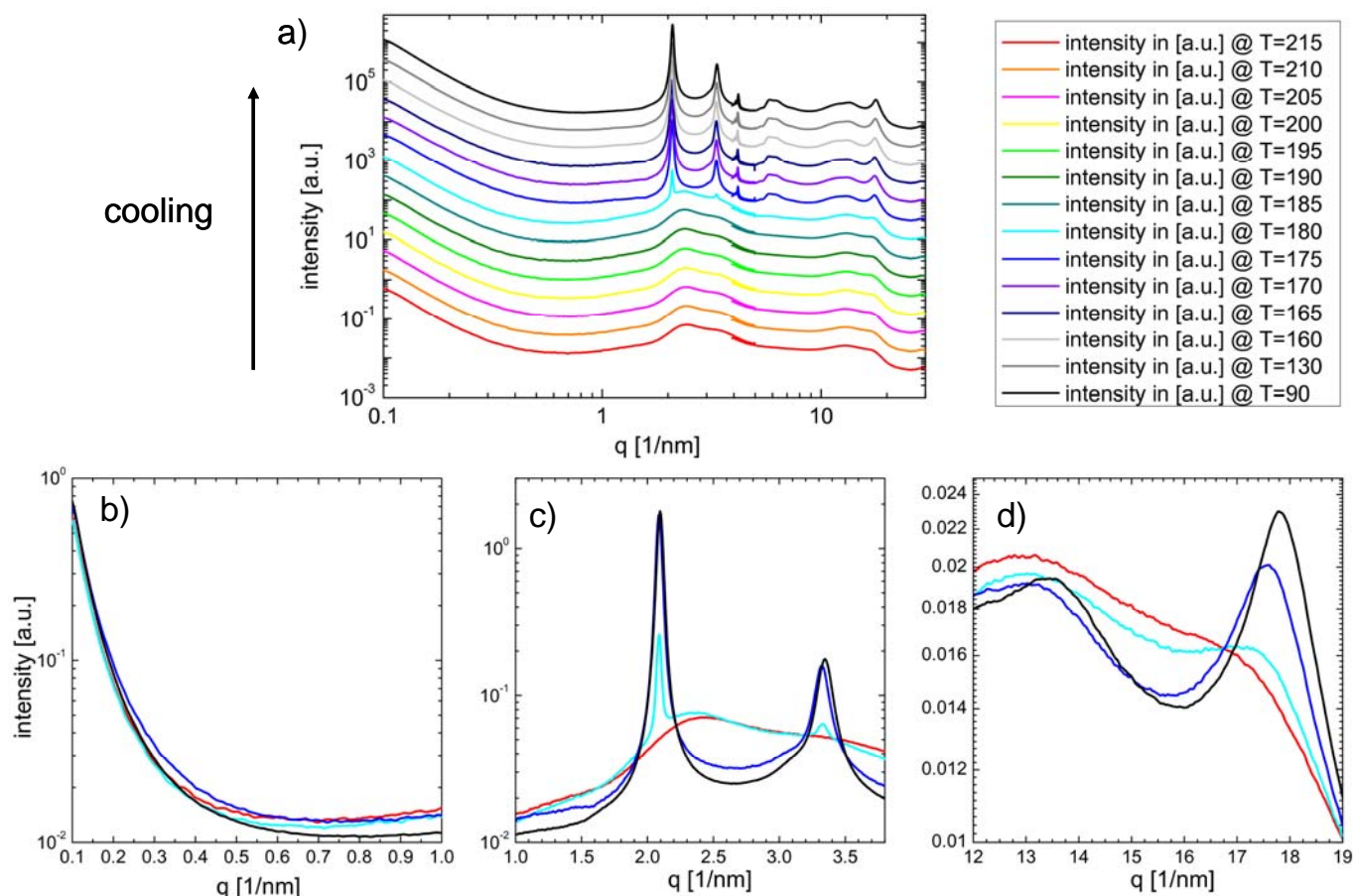


Figure 5. a) Temperature-dependent SAXS/WAXS diffraction pattern of PPerAcr upon cooling from the melt at 10 K/min. b), c), and d) show diffraction pattern at regions in which microphase separation, main-chain/side-chain segregation, and  $\pi$ - $\pi$  stacking, respectively, are observed.

<sup>4</sup> S. M. Lindner, M. Thelakkat, *Macromolecules* 2004, **37**, 8832.

<sup>5</sup> S. M. Lindner, S. Hüttner, A. Chiche, M. Thelakkat, G. Krausch, *Angew. Chem. Int. Ed.* 2006, **45**, 3364.

<sup>6</sup> M. Sommer, S. M. Lindner, M. Thelakkat, *Adv. Funct. Mater.* 2007, **17**, 1493.

<sup>7</sup> M. Sommer, A. Lang, M. Thelakkat, *Angew. Chem. Int. Ed.* 2008, **47**, 7901.



The peak in figure 5d at around  $q \sim 18 \text{ nm}^{-1}$  reflects the  $\pi$ - $\pi$  stacking of the perylene bisimide moieties inside one column (distance 0.35 nm). This distance is almost unchanged compared to low molecular weight systems. The intermediate  $q$ -range (figure 5c) shows two prominent reflections arising from intercolumnar arrangements. The indexing of these peaks is currently under investigation. No structure of the scattering curves in the low  $q$ -region is observed (figure 5b). In this region we will observe reflections when a polystyrene segment is attached to the PPerAcr polymer, as will be shown in the next section.

#### 4) Amorphous-crystalline polystyrene-*block*-poly(peryene bisimide acrylate) PS-*b*-PPerAcr

In the next level of complexity we investigate a block copolymer comprised of PPerAcr and polystyrene. Structure formation will now include the self-assembly of PPerAcr and microphase separation. We seek to investigate how crystallization and microphase separation compete with each other. We investigate several block copolymers PS-*b*-PPerAcr with different compositions and molecular weights. Here we present the results of two block copolymers forming a hexagonally packed cylindrical and a lamellar microphase morphology. Figure 6 shows a series of diffraction patterns of a cylindrical PS-*b*-PPerAcr ( $M_n = 25.8 \text{ kg/mol}$ , wt.-PPerAcr = 65%) during the first cool down at 10 K/min.

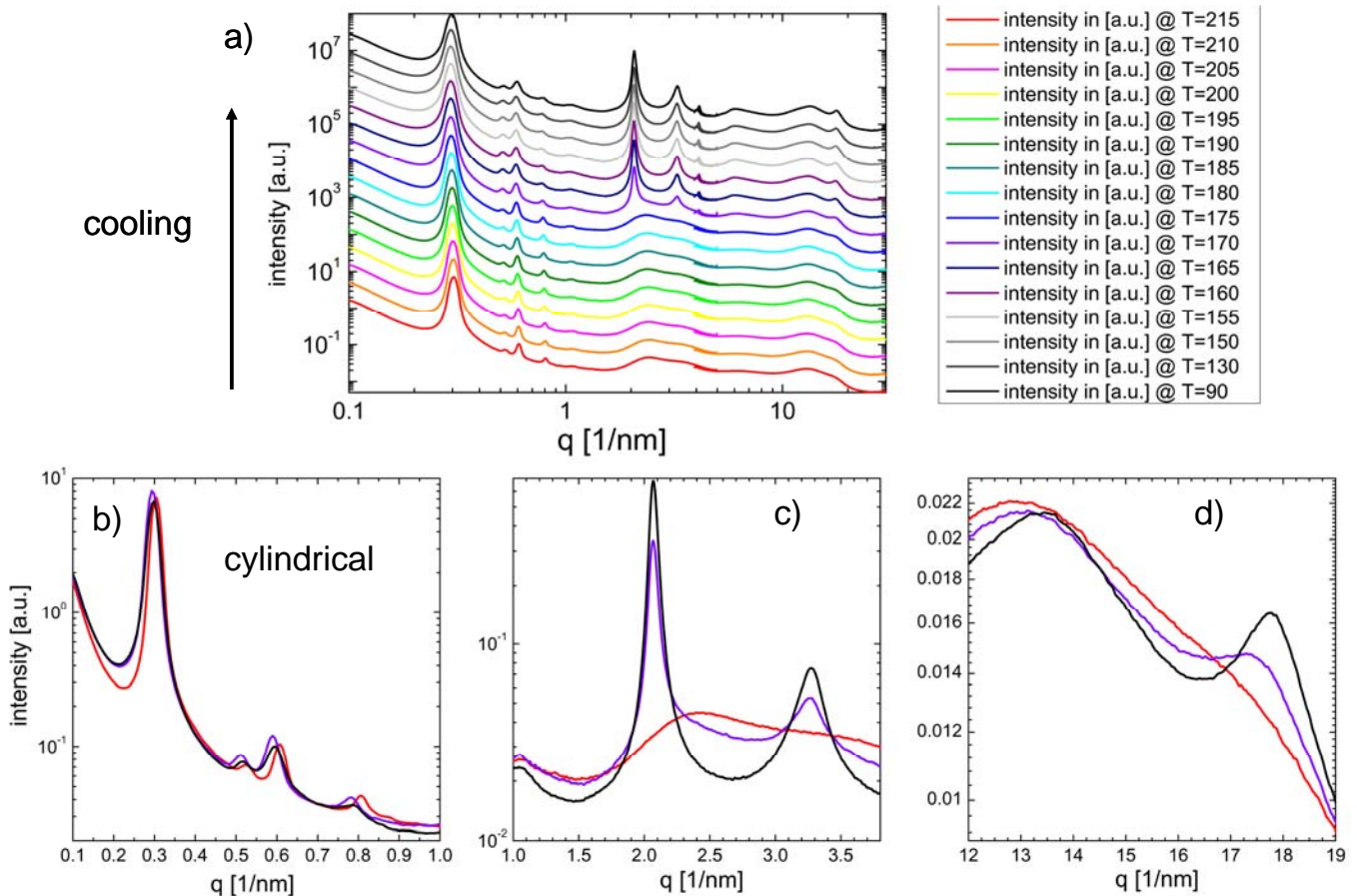


Figure 6. a) Temperature-dependent SAXS/WAXS diffraction pattern of PS-*b*-PPerAcr with 25.8 kg/mol and a PPerAcr weight fraction of 65 % upon cooling from the melt at 10 K/min. b)-d) enlargement of different  $q$ -ranges. b) microphase separation, c) intermediate  $q$ -range of intercolumnar arrangement of the PPerAcr columns d)  $\pi$ - $\pi$  stacking.

We observe sharp peaks and higher order reflections in the low  $q$ -region, which results from the low polydispersity of these materials. PS-*b*-PPerAcr block copolymers on which we have reported earlier<sup>8</sup> exhibited broad PDIs up to 1.8 and broad SAXS reflections. The materials investigated here were purified by preparative GPC and have PDIs between 1.05-1.1. Figure 6b shows the reflections that arise from hexagonal packed cylinders. Within these cylinders, PPerAcr columns are packed (figure 6c). Within the microphase columns, perylene bisimide units still arrange in columns similar to the PPerAcr homopolymer. The  $\pi$ - $\pi$  stacking of the perylene bisimide moieties in PS-*b*-PPerAcr is unaltered in terms of the distance being 0.35 nm. We note that the melt is microphase separated (hexagonal cylinders as well). Crystallization of the PPerAcr segment does not destroy or change the microphase morphology although the PS-segments are mobile at the temperatures where the PPerAcr crystallizes (glass transition temperature of PS is around 100°C).

Figure 7 shows a series of diffraction patterns of a lamellar PS-*b*-PPerAcr ( $M_n$ = 29.9 kg/mol, wt.-PPerAcr = 40%) during the first cool down at 10 K/min. Basically, the same effects are observed compared to the cylindrical PS-*b*-PPerAcr. The melt is microphase separated and this morphology is not altered during crystallization of the PPerAcr segment. The PPerAcr columns are now arranged in a lamellar phase, but apparently the column arrangement is equal compared to the hexagonal cylinder forming block copolymer, as indicated by the intermediate  $q$ -range diffraction peaks.

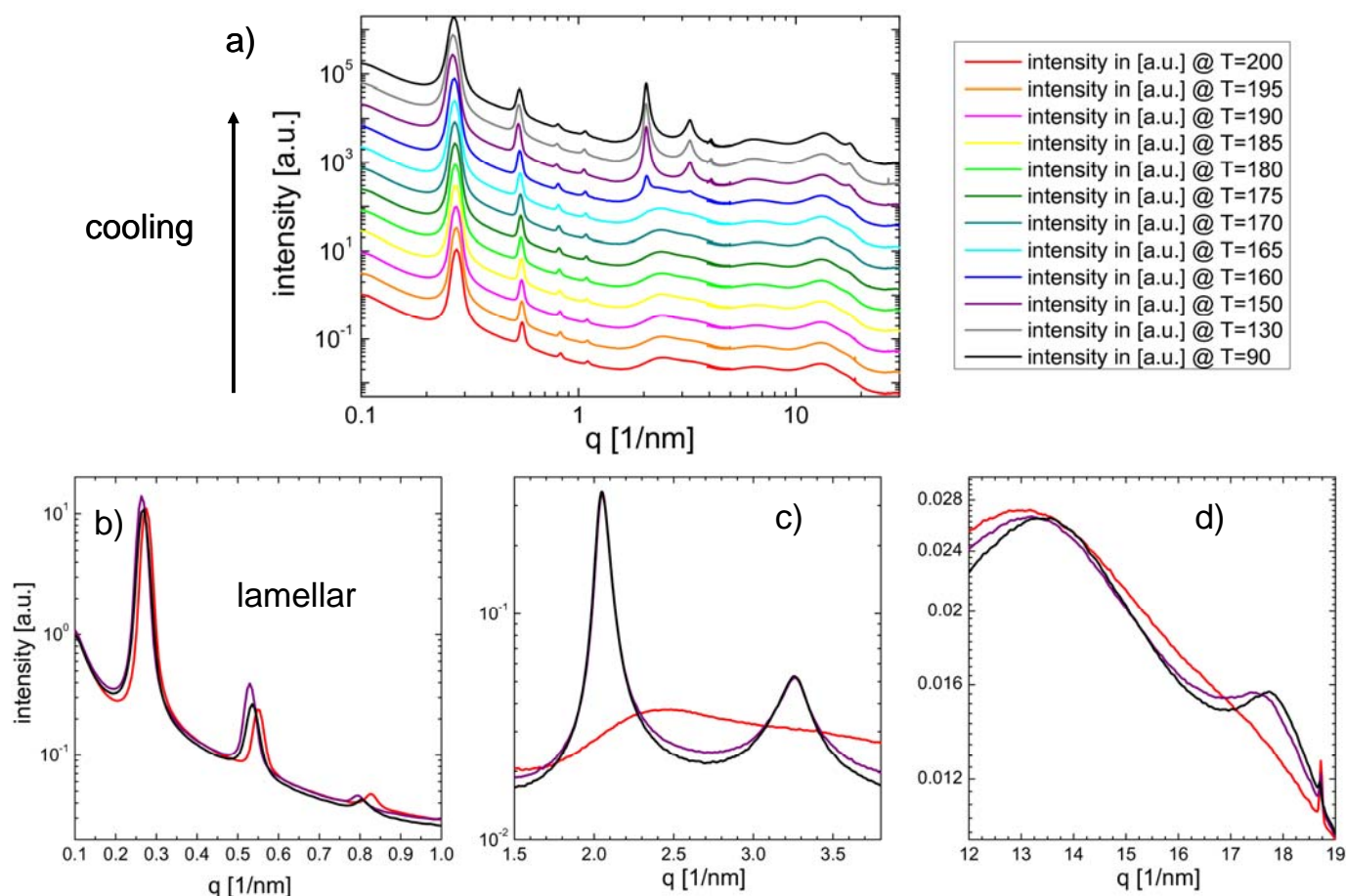


Figure 7. a) Temperature-dependent SAXS/WAXS diffraction pattern of PS-*b*-PPerAcr with 29.9 kg/mol and a PPerAcr weight fraction of 40 % upon cooling from the melt at 10 K/min. b) region of microphase separation, c) region of the first prominent reflection of the PPerAcr columns d)  $\pi$ - $\pi$  stacking.

We conclude that three levels of structural hierarchy are observed in PS-*b*-PPerAcr:  $\pi$ - $\pi$  -stacking, arrangement of columns, and microphase separation. We have found two microphase structures, lamellar and

<sup>8</sup> M. Sommer, S. Hüttner, S. Wunder, *Adv. Mater.* 2008, **20**, 2523.

hexagonal cylinders. The melt microdomain morphologies are equal to the room temperature microdomains. The crystallization inside the microdomains seems not to depend on the geometry of the domain (lamellar or cylindrical).

## 5) Double Crystalline Block Copolymers P3HT-*b*-PPerAcr

Double crystalline block copolymers bear the highest level of complexity among the investigated block copolymers. The polymer consists of a block made of poly(hexylthiophene) P3HT and a PPerAcr block. P3HT belongs to the ubiquitous hole transporting materials for organic solar cells. This system comprises an hole transporting or p-type material, and an acceptor or n-type material, respectively. These materials are intended to be used in organic electronic devices such as photovoltaic devices or organic field effect transistors. This system P3HT-*b*-PPerAcr shows the highest external quantum efficiencies observed so far in block copolymer based photovoltaic cells.<sup>9</sup> The incorporation of the dual functionality into one macromolecule enables the control of the nanomorphology for device improvement, but also offers an ideal system for spectroscopic studies, that establish structure function-relations of these donor-acceptor systems.

A first very important question we could answer during these measurements is the competing crystallization of the two blocks. P3HT as well as PPerAcr are crystalline polymers with similar melting temperatures. Fig. 8 shows the kinetics of crystallization of P3HT-*b*-PPerAcr when cooled down from melt. The comparison of two block copolymers with the same block ratio (55wt% PerAcr) but different molecular weights shows that in case of the low molecular weight block copolymer ( $M_n=16$  kg/mol) PPerAcr block crystallises first (Fig.8a). In case of the higher molecular weight block copolymer ( $M_n=30$ kg/mol) (Fig.8b), almost simultaneous crystallization takes place. Fig. 8c shows the XRD measurements for block copolymers with constant P3HT block length, but different PPerAcr block lengths. The diffraction peaks suggest a square packed cylindrical arrangement of the PPerAcr columns and two crystalline domains – P3HT lamellae and PPerAcr cylinders - are prevalent.

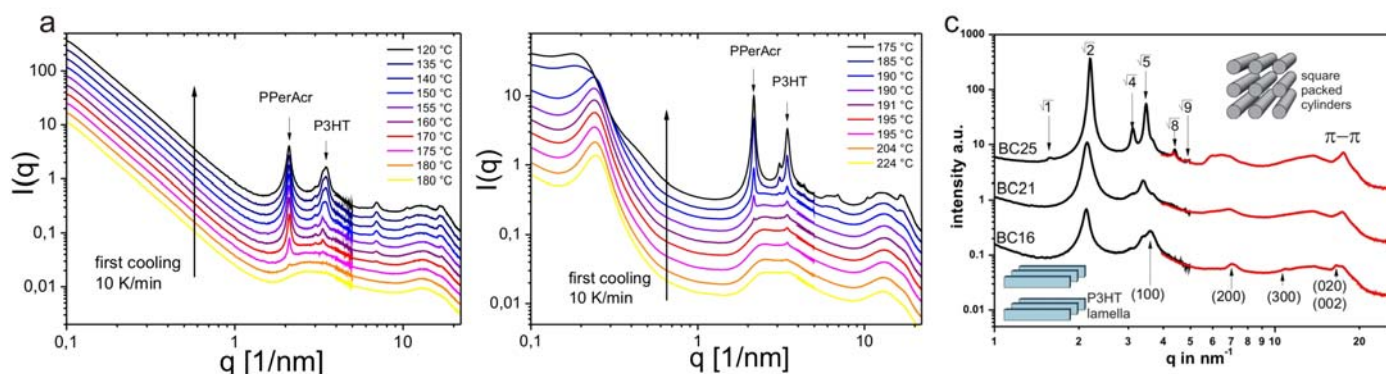


Fig. 8 – a) Temperature dependent XRD-spectra of a P3HT-*b*-PPerAcr block copolymer ( $M_n=16$ kg/mol) on cooling from melt with 10K/min. Under these conditions, the PPerAcr block recrystallises first and the P3HT block shows a stronger undercooling. b) At a higher molecular weight of P3HT-*b*-PPerAcr ( $M_n=30$ kg/mol), the P3HT seems to recrystallise earlier. c) Comparison of different molecular weights of the block copolymer, whereby the P3HT block length is kept constant at ~9 kg/mol. BC 25, the block copolymer with 81wt% content of PPerAcr shows distinct features of a square packed cylindrical mesostructure.

<sup>9</sup> M. Sommer, S. Hüttner, U. Steiner, M. Thelakkat, *Appl. Phys Let.* 2009, in print.



## General conclusions and outlook

The ID02 beamline is perfectly suited for the needs of the materials investigated. This, together with the new sample holder geometry for measuring free-standing bulk samples temperature-dependent and the great success of the session, is an ideal starting point for further measurements. We therefore plan to apply for further beamtime in the future. Therein, we plan to synthesize and measure more block copolymers PS-*b*-PPerAcr to understand the phase diagram in more detail. Another important point is the orientation of the PPerAcr columns inside the microdomains. These two points will be part of future proposals.

Our ultimate goal is the determination of the structure of fully functionalized block copolymers that bear both, hole conducting as well as electron conducting blocks. Thereby, the hole conducting blocks can be either amorphous or crystalline. We have now achieved preliminary temperature-dependent scattering data on such fully functionalized materials. Furthermore, the morphology and structural build-up can be elegantly controlled by solvent vapor annealing techniques, which are much more gentle post-treatment methods than thermal annealing for thin layer devices. Therefore, we plan to carry out *in-situ* solvent vapor annealing for the future SAXS/WAXS measurements in similar systems to gain knowledge about changes in morphology and structures which have strong influence on device performance. Therefore additional beamtime is required for completion of these experiments. We are very satisfied with the first result obtained within this first proposal and look forward to continue this project.